Title

Recombinant Vgr-1/BMP-6-expressing tumors induce fibrosis and endochondral bone formation in vivo.

Journal

The Journal of cell biology, 126(6)

ISSN

0021-9525

Authors

Gitelman, SE
Kobrin, MS
Ye, JQ
et al.

Publication Date

1994-09-01

DOI

10.1083/jcb.126.6.1595

Peer reviewed

Recombinant Vgr-1/BMP-6–expressing Tumors Induce Fibrosis and Endochondral Bone Formation In Vivo

Stephen E. Gitelman,*‡ Michael S. Kobrin, Jian-Qin Ye,*‡ Alfredo R. Lopez,¶ Angela Lee,** and Rik Derynck‡§‖**

Departments of *Pediatrics, ‡Growth and Development, and §Anatomy, ‖Programs in Cell Biology and Developmental Biology, and ¶Hematology/Oncology Section at Veterans Administration Medical Center, University of California at San Francisco, San Francisco, California 94143; and **Genentech, Inc., South San Francisco, California 94080

Abstract. Members of the TGF-β superfamily appear to modulate mesenchymal differentiation, including the processes of cartilage and bone formation. Nothing is yet known about the function of the TGF-β–related factor vgr-1, also called bone morphogenetic protein-6 (BMP-6), and only limited studies have been conducted on the most closely related factors BMP-5, osteogenic protein-1 (OP-1) or BMP-7, and OP-2. Because vgr-1 mRNA has been localized in hypertrophic cartilage, this factor may play a vital role in endochondral bone formation. We developed antibodies to vgr-1, and documented that vgr-1 protein was expressed in hypertrophic cartilage of mice. To further characterize the role of this protein in bone differentiation, we generated CHO cells that overexpressed recombinant murine vgr-1 protein. Western blot analysis documented that recombinant vgr-1 protein was secreted into the media and was proteolytically processed to yield the mature vgr-1 molecule. To assess the biological activity of recombinant vgr-1 in vivo, we introduced the vgr-1–expressing CHO cells directly into the subcutaneous tissue of athymic nude mice. CHO-vgr-1 cells produced localized tumors, and the continuous secretion of vgr-1 resulted in tumors with a strikingly different gross and histological appearance as compared to the parental CHO cells. The tumors of control CHO cells were hemorrhagic, necrotic, and friable, whereas the CHO-vgr-1 tumors were dense, firm, and fibrotic. In contrast with control CHO tumors, the nests of CHO-vgr-1 tumor cells were surrounded by extensive connective tissue, which contained large regions of cartilage and bone. Further analysis indicated that secretion of vgr-1 from the transfected CHO tumor cells induced the surrounding host mesenchymal cells to develop along the endochondral bone pathway. These findings suggest that endogenous vgr-1 acts as an osteoinductive factor during endochondral bone formation.

During development, a variety of growth and differentiation factors influence cell proliferation, differentiation, and migration. Several secreted peptide growth factors have been shown to mediate these processes, exerting their activities locally in an autocrine or paracrine fashion (reviewed in reference 20). The TGF-β superfamily represents one group of such factors that is particularly important in modulating mesenchymal differentiation (reviewed in references 10, 41). This family of factors influences pluripotent progenitor cells to differentiate into fibroblasts, adipocytes, myoblasts, chondrocytes, or osteoblasts. Correctly coordinated differentiation of mesenchymal cells into such cell lineages may depend on a defined spatial and temporal expression pattern for specific TGF-β–related factors (for examples, see references 14, 31).

One aspect of mesenchymal differentiation that remains incompletely characterized includes endochondral bone formation, bone fracture healing, and ectopic bone formation, all of which proceed through a similar developmental cascade. In these processes, mesenchymal precursor cells first differentiate into chondrocytes and give rise to a cartilage template. Within the center of this template, the chondrocytes enter a proliferative phase, then mitosis arrests and the cells undergo hypertrophy. The hypertrophic cartilage mineralizes in the later stages of maturation, and is eventually invaded by blood vessels and replaced by a mineralized bone matrix. This bone matrix is deposited by osteoblasts, which also have differentiated from mesenchymal progenitor cells. Recent evidence implicates TGF-β superfamily members as playing a central role in this complex developmental process (reviewed in references 10, 55).

The TGF-β superfamily consists of a growing number of homologous, secreted, disulfide-bonded dimers (reviewed in

Address all correspondence to Stephen E. Gitelman, Department of Pediatrics, University of California at San Francisco, Box 0136, Millberry Union East, Room 405, San Francisco, CA 94143. Phone: (415) 476-3748; fax: (415) 476-1343. The present address for Michael S. Kobrin is Departments of Medicine and Biological Chemistry, University of California, Irvine, CA 94305-5487. The present address for Angela Lee is Department of Immunology, Stanford University School of Medicine, Palo Alto, CA 94305-5487.

references 10, 41). These proteins can be further subdivided into several groups, based on sequence homology. One of these groups consists of the three TGF-β isoforms, TGF-β1, -β2, and -β3. Other distinct groups include the activins, inhibins, and Müllerian inhibitory substance. However, by far the largest group comprises the bone morphogenetic proteins (BMPs)[1], *Xenopus* vg-1, *Drosophila* decapentaplegic (dpp), and the more recently cloned polypeptides nodal (59), dorsalin (3), vgr-2 (22), and growth/differentiation factors (GDF)-1 (27) and GDF-3 (33). This group has been referred to as the decapentaplegic/vg-1–related proteins (DVR) (30).

The TGF-β superfamily, and especially the DVR group, appears to be of considerable importance in bone and cartilage development. Several members of this superfamily have been localized during intramembranous and endochondral bone formation, and they are expressed in a spatially and temporally distinct but overlapping pattern in the differentiating tissue (for an example, see reference 31). The proteins that have been best characterized in terms of their osteoinductive activity are the subgroup consisting of BMP-2 and BMP-4 (reviewed in reference 55), which bear closest homology with the decapentaplegic complex protein dpp of *Drosophila* (38). BMP-2 and BMP-4 have the ability to induce osteoblastic differentiation in vitro and ectopic bone formation when injected intramuscularly (for examples, see references 6, 17, 18, 24, 49, 51, 56, 57), and are at least partially responsible for the osteoinductive activity originally purified from bone (40, 46).

The largest subgroup of DVR proteins consists of BMP-5 (5), vgr-1 (29) or BMP-6 (5), osteogenic protein-1 (OP-1) (36) or BMP-7 (5), and OP-2 (37), all of which have a high degree of homology to the ancestral 60A protein in *Drosophila* (12). Although BMP-7 has been shown in an initial study to induce bone formation in vivo (43) and osteoblastic and chondrocytic differentiation in vitro (1, 43), little is currently known about the functions of the other members of this subgroup and their expression patterns during mammalian development. To define the function of this subgroup in mesenchymal differentiation and especially during endochondral bone formation, we have selected vgr-1/BMP-6 as a prototype for our studies. This cDNA was originally isolated from a murine embryonic cDNA library and was named vgr-1, based on its homology with *Xenopus* vg-1 (29). The human and bovine homologues of vgr-1 were subsequently cloned from bone and were named BMP-6 (5), but no bone morphogenetic activity has been reported for this protein. Extensive in situ hybridization analyses have localized vgr-1 mRNA expression to the central nervous system, to various epithelial structures including the suprabasal layer of the epidermis, and, of most relevance to the current studies, to hypertrophic cartilage (21, 31). Notably, it is the only member of the TGF-β superfamily that has been localized to hypertrophic cartilage, and, as such, vgr-1 protein could be involved in the maturation of hypertrophic cartilage and/or stimulation of osteoblastic differentiation. However, in a recent immunohistochemical localization study, vgr-1 protein was not detected in hypertrophic cartilage, suggesting that there may be translational inhibition of vgr-1 expression in the latter tissue (50).

1. *Abbreviations used in this paper:* BMPs, bone morphogenic proteins; dhfr, dihydrofolate reductase; dpp, decapentaplegic; DVR, dpp/vg-1–related proteins; GDF, growth/differentiation factors; OP-1, osteogenic protein-1.

In this study, we developed antibodies to vgr-1, and showed that vgr-1 protein was indeed expressed in hypertrophic cartilage. Furthermore, we generated transfected CHO cells that produced recombinant vgr-1 protein, and showed that the protein was proteolytically processed and secreted by these cells. Injection of the vgr-1–expressing CHO cells into the subcutaneous tissue of nude mice resulted in tumors with fibrosis and regions of cartilage and bone. Further analysis indicated that vgr-1 secreted by the injected CHO cells induced the surrounding host mesenchymal cells to differentiate into chondrocytes and osteoblasts. Our data indicate that vgr-1 may represent a vital factor for differentiation along the endochondral bone cascade.

Materials and Methods

Construction of the vgr-1 Expression Vector

To obtain the vgr-1 gene, a 780-bp SmaI fragment from the 5′ end of the vgr-1 cDNA was used as a probe to screen a mouse genomic library in λ Charon 4A under high stringency. The library was plated at 50,000 pfu/plate, and ~1 × 10^6 clones were screened. Candidate positive clones from duplicate filter lifts were purified through subsequent rounds of screening. Library plating, probe labeling, phage lifts, and filter hybridizations were carried out as described previously (11). Restriction fragments of one such phage were subcloned into pUC219 for further mapping, and subsequently sequenced in M13 through standard dideoxy sequencing (44) with Sequenase (United States Biochemical Corp., Cleveland, OH). This analysis led to the identification of the first coding exon of the vgr-1 gene.

For expression studies, the original vgr-1 cDNA (29) was subcloned into the BamHI-EcoRI site of the pRK7 expression vector (53). To generate the composite full-length vgr-1 cDNA expression vector, we replaced the 5′ coding sequence of the original cDNA (29) with an 851-bp BamHI/BspHI genomic fragment that contained 5′ flanking DNA and the first coding exon, and then performed a three-part ligation in which this fragment was ligated with the downstream 1551-bp BspHI/EcoRI 3′ vgr-1 cDNA fragment and the pRK 7 expression vector that had been digested with BamHI and EcoRI. The resultant plasmid was named pRK7-vgr-1.

Cell Culture and Transfection

CHO cells deficient in the synthesis of dihydrofolate reductase (dhfr) (47) were propagated in F-12 Ham's nutrient mix (Gibco BRL, Gaithersburg, MD) and supplemented with 10% fetal calf serum (Hyclone Laboratories, Logan, UT), 100 U/ml penicillin, and 100 μg/ml streptomycin (both from Gibco BRL). Cells were transfected with 15 μg of the pRK7-vgr-1 expression vector and 300 ng of pSV-dhfr DNA (45) using the calcium-phosphate precipitation method (52). Cells were incubated for 4 h, the medium was removed, and the cells were exposed to a 15% glycerol shock for 1 min. After rinsing twice with PBS, the cells were incubated in supplemented media until they reached confluence, at which time they were split 1:8 and selected in media lacking glycine, hypoxanthine, and thymidine, and supplemented with 5% dialyzed fetal calf serum. Individual clones were selected after 3 wk, and, after expansion, were screened by Northern blot analysis for expression of vgr-1 mRNA. The integrated plasmid sequences of several positive clones were amplified through culturing in gradually increasing levels of methotrexate, up to 500 nM, thereby generating the CHO-vgr-1 cells.

Transient transfections of pRK7-vgr-1 into 293 cells were performed as described previously (15).

RNA Preparation and Northern Blot Analysis

Total RNA was prepared from cultured cells by lysis with guanidinium isothiocyanate, phenol extraction, and ethanol precipitation, according to standard protocols (7). The RNA was quantitated spectrophotometrically at 260 nm, and was stored at −70°C until use. For Northern blot analysis, 20 μg of total RNA was electrophoresed in a formaldehyde gel in MOPS buffer and transferred to nylon membranes (Gene Screen; New England Nuclear, Boston, MA). The vgr-1 cDNA probe corresponded to the 2.4-kb BamHI/EcoRI cDNA from the pRK7-vgr plasmid, and was radiolabeled using the [^{32}P]dCTP random primer labeling method (Oligolabeling Kit;

Pharmacia, Uppsala, Sweden). Hybridization, washing, and autoradiography were performed as described previously (14).

Cell Growth Rate

CHO or transfected CHO-vgr-1 cells were rinsed with PBS, trypsinized in 0.25% trypsin with 0.02% versene, and diluted in standard media. The cell number was determined using a Coulter counter (Coulter Corp., Hialeah, FL), and 10,000 cells were plated per well on 24-well plates. The cells were grown in standard media with 10% fetal calf serum. For analysis of growth rate in the presence of serum, the wells were rinsed, trypsinized, and counted at regular intervals starting 12 h after initial plating. For each time point, three separate wells of cells were individually counted three times, and the cell number was then averaged. For analysis of growth rate in the absence of serum, the freshly plated cells were grown in 10% fetal calf serum for 24 h, then the cells were rinsed three times with PBS and subsequently grown in media supplemented with insulin, transferrin, and selenium (GMS-G supplement; Gibco-BRL). The cells were again grown in triplicate for each time point, and were first counted 24 h after the serum had been withdrawn.

Antibody Production

Oligopeptides were synthesized corresponding to the deduced murine protein sequence at amino acids 141-157 for the pro region antibody and 392–407 for the mature region antibody (see Fig. 2). No similar sequences are present in BMP-5 and BMP-7, and therefore no crossreactivity was expected between the vgr-1 antibodies and these BMPs. An additional cysteine residue was added to the amino terminus of each oligopeptide. The peptides were coupled to keyhole limpet hemocyanin according to the method of Green et al. (16), and were then mixed in Freund's adjuvant and injected into rabbits (Caltag Laboratories, Inc., South San Francisco, CA). Two animals were injected with each antigen. The initial injection consisted of 150 μg in Freund's adjuvant with subsequent booster doses of 100 μg 3 and 4 wk from the initial injection. The first bleed occurred at 5 wk from the initial injection. A 100-μg injection was given after that bleed, and follow-up bleeds and injections were each performed at weekly intervals for the next 2 wk, and with a last bleed 1 wk later. There was a 2-wk rest period, then weekly booster injections for 2 wk, followed by a repetition of the above cycle. Antisera was stored at −20°C until use.

Whole antisera was used for Western blot analysis at the dilutions noted below. For immunohistochemistry, the antisera were first purified by passage over the appropriate antigen affinity column. The columns were constructed by coupling of the synthetic oligopeptides to Affigel-10 (Bio Rad, Laboratories, Richmond, CA) according to manufacturer's instructions. The antisera was purified by mixing with an equal volume of 0.1 M PBS (pH 7.2) and loading onto the appropriate affinity column that had been preequilibrated with this buffer. The column was washed with PBS until the eluant achieved a baseline reading at OD_{280nm}. The specific anti-vgr-1 antibodies were then eluted with 40 mM diethylamine (pH 11.4), and exchanged into PBS buffer by passage over a YM-10 membrane (Amicon Corp., Beverly, MA).

Western Blot Analysis

Conditioned media was collected from CHO or CHO-vgr-1 transfectants grown in media in the absence of serum for 24 h. 200-μl aliquots were lyophilized to dryness, and were resuspended in sample buffer under reducing conditions with 5% β-mercaptoethanol. After SDS-PAGE, the samples were transferred to nitrocellulose. Immunoblotting was performed with the enhanced chemiluminesence kit (Amersham Corp., Arlington Heights, IL) according to manufacturer's recommendations. Whole antisera directed against the precursor oligopeptide were used at a 1:1000 dilution, and that derived from the mature oligopeptide was used at a 1:250 dilution. Incubations with the antibodies were performed overnight at 4°C.

Injections into Nude Mice

Homozygous nude, athymic 30-g female mice were obtained from Charles River Laboratories (Wilmington, MA). 5×10^6 CHO or CHO-vgr-1 cells were injected into the right paraspinous area in the lower lumbar region. Cells were prepared for injection by trypsinization, multiple washes with PBS, and resuspension in 0.5 ml of serum-free media per sample. The animals were fed ad libitum and monitored three times per week for the appearance of solid tumors. When the tumors reached 4 cm in largest diameter, or by 4 wk, the animals were euthanized, and the tumors were resected. Portions of the tumors were fixed in 4% paraformaldehyde and embedded in paraffin. The remainder were placed in Tissue Tek OCT compound (Miles Inc., Elkhart, IN) and snap frozen in liquid N_2.

Histochemistry and Immunohistochemistry

5-μm paraffin sections were used for all histochemical analyses, and all staining was performed according to standard procedures (8).

For immunocytochemistry, cells were grown on tissue culture chamber slides (Nunc Inc., Naperville, IL) to 80% confluence, washed with PBS, fixed in methanol for 10 min, and then stored at −70°C. After several PBS rinses, endogenous peroxidase activity was quenched with 0.3% H_2O_2 in 10% methanol for 20 min. The slides were again rinsed in PBS and blocked with 3% BSA in PBS for 30 min at room temperature. The primary antibodies were then applied and incubated overnight at 4°C. The affinity-purified vgr-1 precursor antibody was used at a 1:50 dilution (8 μg/ml). After washes with PBS-0.1% Tween 20, anti-rabbit IgG horseradish peroxidase (Amersham Corp.) was applied at a 1:1000 dilution for 60 min at room temperature. After further washes, 3-amino-9-ethylcarbazole (AEC) substrate (Dako Co., Carpinteria, CA) was added for 5 to 10 minutes, and then the slides were washed in de-ionized H_2O, counterstained with hematoxylin, and washed with tap H_2O.

For analysis of vgr-1 expression in histological sections, we collected mice from gestational day 18.5 embryos, fixed the tissue in 4% paraformaldehyde for 30 minutes, and used 5 μm sections for immunostaining. The affinity-purified mature vgr-1 antibody was used at a 1:50 dilution (6 μg/ml). For analysis of the tumors, we used sections from tumors that had been snap frozen in liquid N_2 following embedding in Tissue Tek OCT Compound. The collagen type I antibody was an affinity purified goat antibody raised against human and bovine antigens, and the collagen type II antibody was an affinity-purified antibody directed against the bovine antigen (both antibodies from Southern Biotechnologies, Inc., Birmingham, AL). Both antibodies were used at dilutions of 1:1,500. The monoclonal murine osteocalcin antibody was purchased from Biomedical Technologies, Inc. (Stoughton, MA), and was used at a 1:200 dilution.

In Situ Hybridization

To evaluate the expression of dihydrofolate reductase, we used the 548-bp BamHI/BglII fragment from the 3′ untranslated region of the hepatitis B surface antigen gene, which had been incorporated into the 3′ region of the dihydrofolate reductase expression unit (45). This fragment was cloned into the Bluescript vector (Stratagene, La Jolla, CA), and sense and antisense riboprobes were generated with [^{35}S]UTP and T3 and T7 RNA polymerases, respectively, according to the supplier's protocols (Promega Corp., Madison, WI).

Frozen sections of 5 μm were cut onto "probe-on plus" microscope slides (Fisher Scientific, Pittsburgh, PA), and stored at −70°C. The sections were fixed in paraformaldehyde, acetylated, and prehybridized essentially as described previously (34). Prehybridization was performed at 50°C in hybridization buffer for 1 h, and then the solution was removed and replaced with the same buffer containing 1×10^6 cpm of riboprobe, and incubated for 16 h at 50°C. Posthybridization washes and RNase treatments were carried out as noted previously (34). After washes, the slides were dehydrated in increasing concentrations of ethanol with 0.3 M ammonium acetate, air dried, and dipped into Ilford Nuclear Research Emulsion (Cheshire, United Kingdom). Sections were exposed in light safe boxes at 4°C for 6 d, and then developed in D-19 developer (Eastman Kodak, Rochester, NY). The slides were counterstained in Harris' hematoxylin, and then analyzed under bright-field and dark-field microscopy.

Results

Vgr-1 Protein is Expressed in Hypertrophic Cartilage

Previous in situ hybridization studies have documented expression of vgr-1 mRNA in the central nervous system, various epithelial structures including the suprabasal layer of skin, and hypertrophic cartilage (21, 31). Wall et al. recently developed an antibody directed against the precursor region of the murine vgr-1 protein, and subsequent immunohistochemical analysis in the developing mouse confirmed the presence of vgr-1 protein in the central nervous system

and various epithelial structures (50). However, this antibody failed to detect vgr-1 protein expression in hypertrophic cartilage and in some cell lines that express vgr-1 mRNA, suggesting that there was translational control of vgr-1 expression. Thus, before proceeding with our studies on the role of vgr-1 in endochondral bone formation, we had to determine if vgr-1 protein was even present in hypertrophic cartilage. Towards this end, we developed polyclonal antibodies that specifically recognized both the precursor and mature portions of the murine vgr-1 protein.

No purified vgr-1 protein was yet available for antibody production. Instead, we synthesized two oligopeptides from the deduced murine vgr-1 cDNA sequence for use as immunogens. These peptides were selected from regions that have no similarity with the corresponding sequences of the most closely related factors BMP-5 and -7 (5), and thus the resultant antibodies should not cross-react with any related DVR-like factor. Oligopeptides corresponding to amino acids 141-157 in the precursor and 392-407 in the mature portion of the vgr-1 protein (see Fig. 2) were synthesized, coupled to keyhole limpet hemocyanin, and were then used as immunogens in rabbits. Antisera exhibited high titers in ELISA assays with these peptides, and reacted in Western blot assays with recombinant vgr-1 protein synthesized by transfected CHO cells (see below). The whole antisera were then affinity purified using the appropriate immunogenic oligopeptide coupled to Affigel as an affinity matrix, and they yielded antibodies suitable for immunohistochemical analyses of vgr-1 expression.

Immunostaining using the antibody raised against the mature, carboxy-terminal portion of the protein detected vgr-1 protein in the suprabasal layer of the epidermis (see Fig. 1, *A* and *B*), as described previously (50). In addition, and of importance to our study, we detected vgr-1 protein in hypertrophic cartilage (Fig. 1, *A* and *C*). This staining was predominantly in the extracellular matrix surrounding the hypertrophic chondrocytes. Furthermore, vgr-1 protein localized specifically to regions of hypertrophic cartilage that had undergone mineralization, as shown by corresponding von Kossa staining in an adjacent tissue section (Fig. 1 *D*). Thus, vgr-1 protein appeared in the latter stages of hypertrophic cartilage differentiation. The negative control, performed with substitution of rabbit IgG as the primary antibody, resulted in no such staining pattern, demonstrating the specificity of the vgr-1 immunostaining. When using the antibody raised against the precursor segment peptide, vgr-1 protein was again detected in skin, but only very weak immunostaining was apparent in hypertrophic cartilage (data not shown).

Expression of Recombinant Vgr-1 Protein by Transfected Cells

The expression of vgr-1 in the hypertrophic cartilage suggested that it may play a role in the maturation of the hypertrophic chondrocytes and/or may stimulate new bone formation. However, to date, no natural vgr-1 protein has been purified, and thus nothing is known about its physiological activities. Therefore, to determine the role of this factor in endochondral bone formation, it was necessary to first produce recombinant vgr-1 protein.

Initially, the published vgr-1 cDNA (29) was inserted downstream of the cytomegalovirus promoter in the expression vector pRK7. However, transfections of this expression vector into 293 cells did not result in detectable vgr-1 protein expression. Inspection of the predicted vgr-1 polypeptide sequence showed that the NH_2-terminal sequence did not comply well with the consensus rules of von Heijne for signal peptides (48), and we suspected that our cDNA clone was partial length. We subsequently screened a murine genomic library with a 5′ vgr-1 cDNA probe, and identified an upstream exon that contained the 5′ untranslated region, a translational initiation consensus sequence (26), and a canonical signal peptide sequence (48). Primer extension experiments, using RNA from PYS cells, verified that this sequence represented the 5′ end of the vgr-1 mRNA (Kobrin, M. S., unpublished data). Furthermore, the polypeptide sequence deduced from this genomic fragment now had a high degree of sequence similarity with the NH_2 terminus of bovine BMP-6 (5). In retrospect, we believe that the different 5′ end in the published mouse vgr-1 sequence (29) resulted from a cDNA artifact that is likely related to the high G-C content of this sequence. We then constructed a composite vgr-1 expression vector in pRK7 by ligating a 5′ 851-bp BamHI-BspHI genomic fragment onto the corresponding downstream vgr-1 cDNA fragment (29). Transient transfections of the pRK7-vgr-1 plasmid into 293 cells and metabolic labeling of the proteins now resulted in the appearance of an overexpressed protein consistent in size with the vgr-1 protein (data not shown). The full-length cDNA sequence encoding the 510–amino acid murine vgr-1 polypeptide is shown in Fig. 2.

To produce a stable source of recombinant vgr-1 protein, we cotransfected pRK7-vgr-1 and a dihydrofolate reductase expression plasmid into CHO cells, selected several clones expressing high levels of vgr-1 mRNA, and amplified its expression in the presence of increasing concentrations of methotrexate. As shown in Fig. 3 *A*, Northern blot analysis revealed a high level of vgr-1 mRNA in one such clone grown in 500 nM methotrexate. In contrast, CHO cells transfected with dihydrofolate reductase alone did not express vgr-1 mRNA. Immunostaining using the vgr-1 antiserum also showed specific staining of the vgr-1 mRNA–overproducing CHO-vgr-1 cells, indicating the synthesis of vgr-1 protein (Fig. 3 *C*). The parental CHO cells exhibited no such staining, again indicating lack of vgr-1 expression.

To assume biological activity, members of the TGF-β superfamily must enter the secretory pathway and undergo a proteolytic cleavage that separates the precursor region from the biologically active carboxy terminal domain. To determine if such processing occurs in the CHO-vgr-1 stable transfectants, we collected conditioned media produced by these cells and performed Western blot analyses using our vgr-1 antisera (Fig. 3 *B*). After denaturing gel electrophoresis under reducing conditions and Western analysis, each antiserum recognized two protein bands from the media of transfected cells, but not of the nontransfected cells. The larger protein band had a size of ~69 kD, and it reacted in Western blots with antisera raised against both the precursor and mature vgr-1 segments. This band most likely corresponded to the uncleaved vgr-1 precursor polypeptide, given its dual antibody reactivity and its size. Two lower protein bands were seen as well: a 46-kD protein that reacted only with the antibody specific for the vgr-1 precursor segment, and a 23-kD protein that reacted with the antibody for mature vgr-1. These proteins thus corresponded to the two

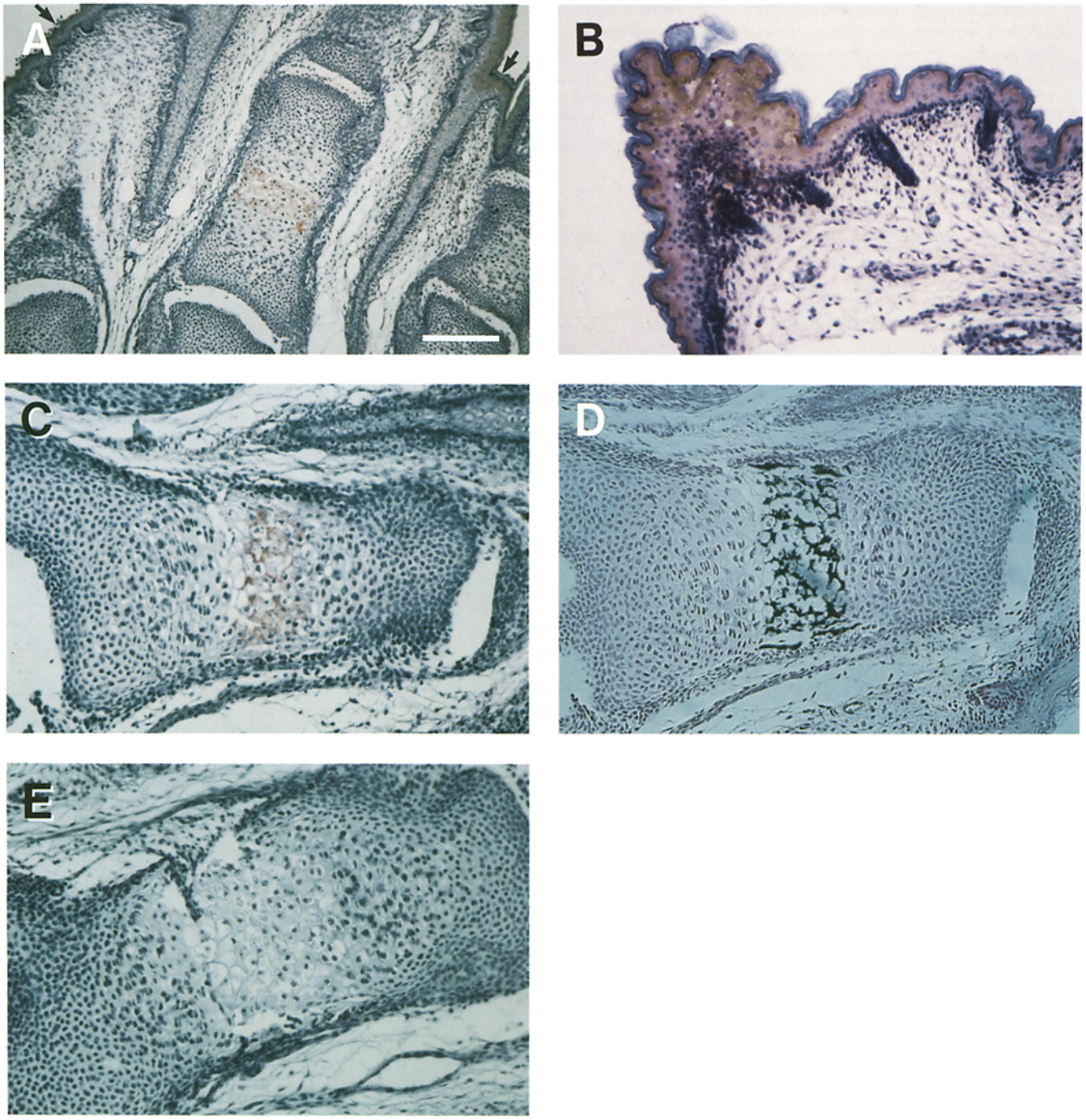

Figure 1. Vgr-1 protein expression in skin and hypertrophic cartilage. Forelimbs from 18.5-d gestation mice were stained with affinity-purified antibody directed against the mature portion of vgr-1. (*A*) ×10 view showing vgr-1 expression in both suprabasal layer of epithelium (*arrows*) and hypertrophic cartilage (*center of figure*). Bar, 200 μm (*B*) ×20 view of the skin showing localization of vgr-1 to suprabasal layer of epithelium. (*C*) ×20 view of vgr-1 expression in hypertrophic cartilage (*center*). (*D*) Section adjacent to that used for *C*, with von Kossa stain (*black*) indicating areas of mineralization, and counterstained with nuclear fast red. (*E*) Negative control, where nonspecific IgG is used as the primary antibody.

cleavage products expected after proteolytic processing of the vgr-1 precursor. These cells secreted ~2 μg/ml per 24 h of the recombinant factor, and based on these Western analyses, ~50% of the secreted protein had been proteolytically processed. The 69- and 46-kD bands each migrated as a subtle doublet (Fig. 3 *B*), which was most apparent in lower percentage polyacrylamide gels (data not shown). This may have been caused by variations in glycosylation.

Effects of vgr-1 on CHO Cells in Culture

To determine the effect of vgr-1 overexpression on these cells, we characterized changes in morphology, growth rate, and collagen synthesis. No significant difference in cell size, shape, or adherence was noted between CHO and CHO-vgr-1 cells (Fig. 3 *C*). However, in comparison with the parental CHO cells, CHO-vgr-1 cells had a significantly slower rate

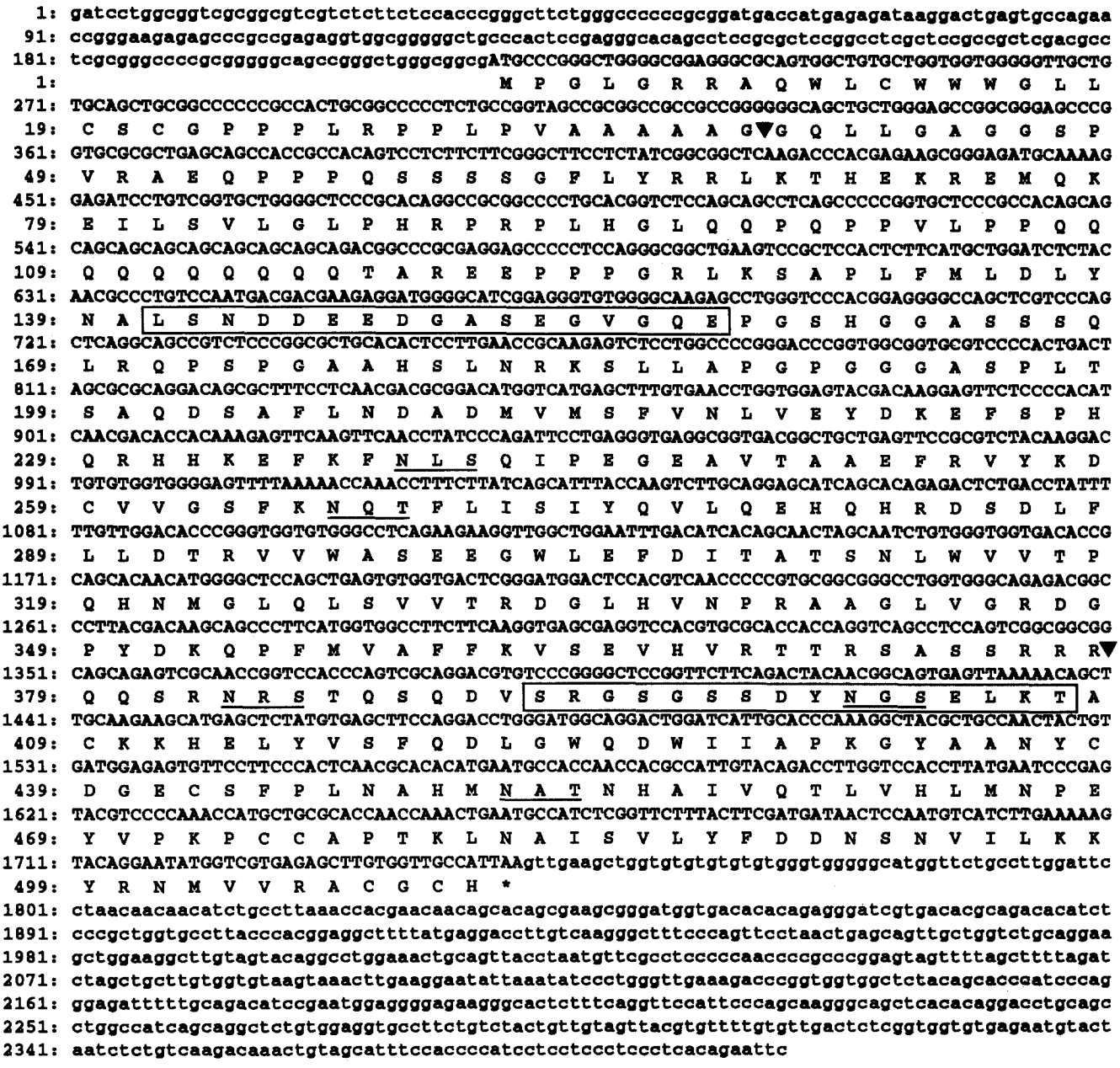

Figure 2. Nucleotide and deduced amino acid sequence of composite vgr-1 cDNA. The 5′ 851 bp are derived from a BamHI/BspHI genomic fragment, and the downstream 1551 bp are from previous vgr-1 cDNA cloning (29). Nucleotide and amino acid numbering is shown in the left column. Untranslated nucleotides are in lowercase lettering. Oligopeptides used for antibody production are boxed, and potential N-linked glycosylation sites are underlined. Potential cleavage sites for eliminating the signal sequence (48) and for separating precursor from mature domains are marked with inverted arrowheads. The stop codon is marked with an asterisk. The nucleotide and protein sequence data reported in this paper will appear in the EMBL Database under the accession number X80992.

of cell proliferation both in the presence and absence of serum (Fig. 4). There were no differences in levels of expression of collagen I and II, as assessed by immunocytochemistry and Northern blot analysis (data not shown).

Vgr-1–expressing CHO Cells form Tumors with Altered Phenotype

To evaluate the effects of vgr-1 in vivo, we injected the vgr-1–expressing CHO cells subcutaneously into nude mice. Previous studies had shown that CHO cells form localized tumors when injected subcutaneously into nude mice (for an example, see reference 13), and we reasoned that the continuous release of recombinant vgr-1 by the tumor cells would allow us to evaluate the biological activity of vgr-1 in vivo. This approach would thus not necessitate the purification of recombinant vgr-1, but would rely on a continuous release of vgr-1 that was naturally activated and incorporated into the extracellular matrix. To this end, we injected CHO or CHO-vgr-1 cells into the right paraspinous area in the lower lumbar region of nude, athymic mice. Five animals were injected with the parental cells, and five with the stable transfected CHO-vgr-1 cells. One animal from each group

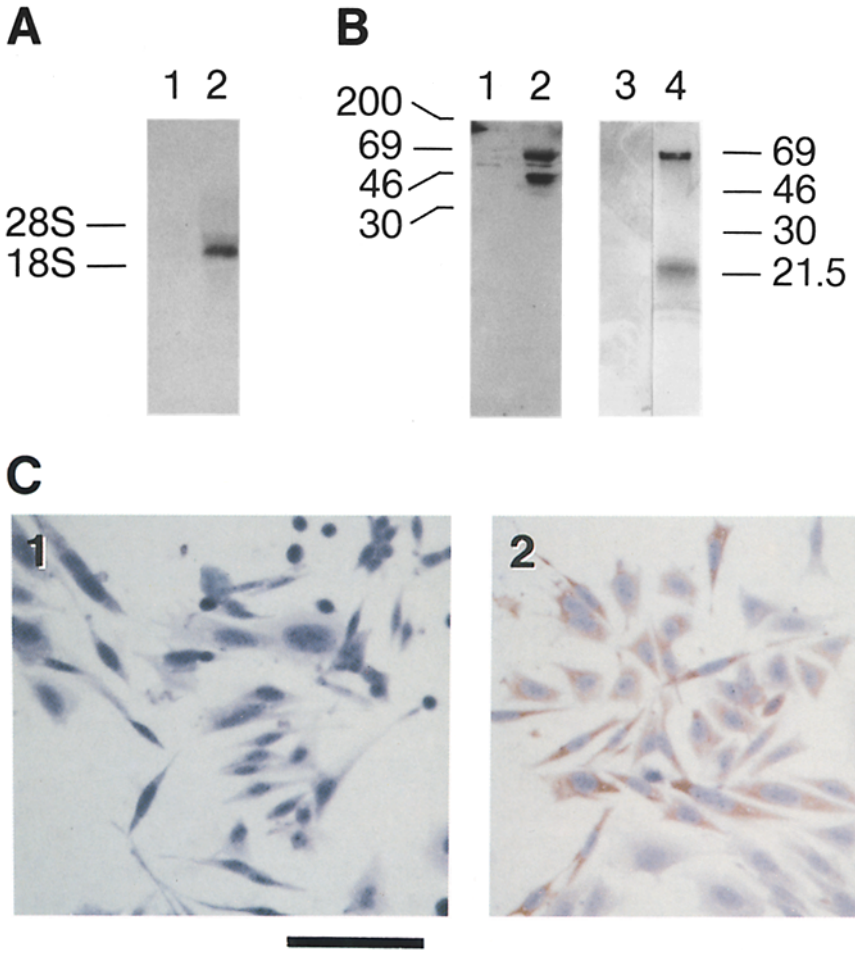

Figure 3. Characterization of CHO-vgr-1 stable transfectants. (*A*) Northern blot analysis of total RNA from CHO (lane *1*) and CHO-vgr-1 cells (lane *2*) after hybridization with vgr-1 cDNA and stringent washing. The positions of 28S and 18S ribosomal RNA are marked. (*B*) Western blot analysis of conditioned media from CHO (lanes *1* and *3*) and CHO-vgr-1 cells (lanes *2* and *4*) incubated with either antisera directed against the vgr-1 precursor segment (lanes *1* and *2*) or mature vgr-1 protein (lanes *3* and *4*). Protein standards are noted. (*C*) Immunostaining of (*1*) CHO and (*2*) CHO-vgr-1 transfectants with affinity-purified vgr-1 antibody directed against the precursor portion of the molecule. Bar, 100 μm.

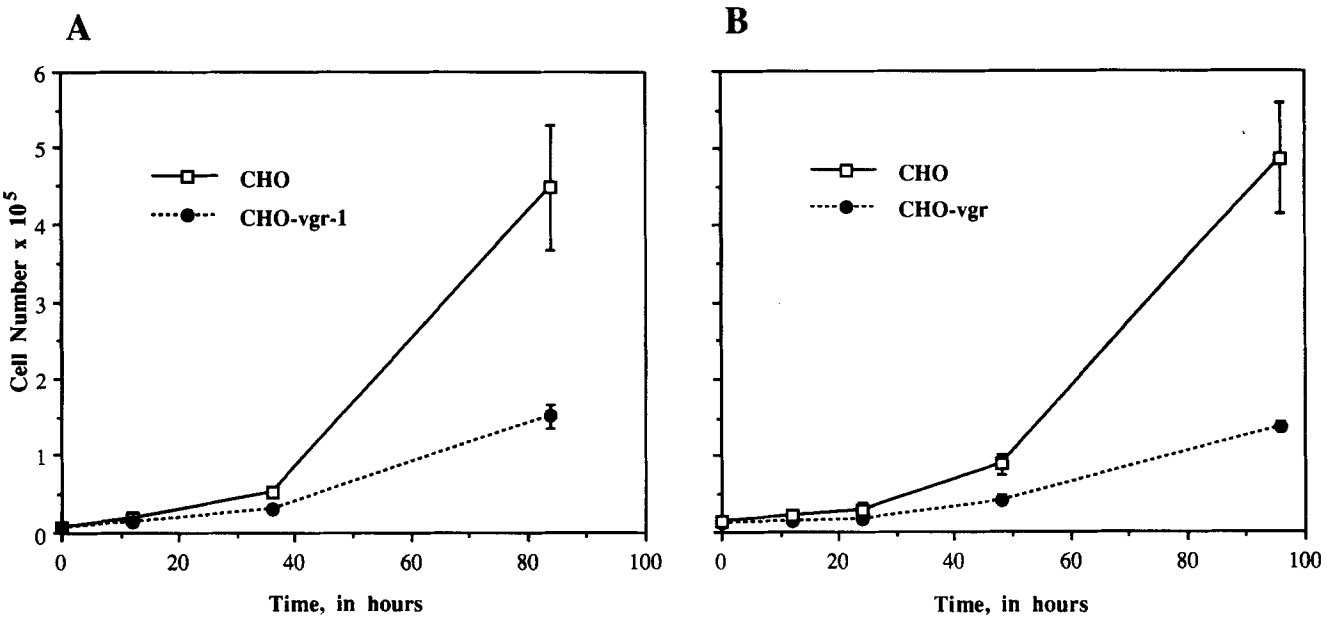

Figure 4. Growth rate of CHO vs CHO-vgr-1 transfectants. Cells were grown in either 10% fetal calf serum (*A*) or in insulin, transferrin, and selenium (*B*). The growth of CHO cells is represented by the full line with open symbols, and CHO-vgr-1 cells are noted by the dashed line with closed symbols. Three independent plates were grown for each cell type under each condition at each time point, and each plate was counted individually three times and then averaged. Each point on the graph represents the average of these readings, with standard deviation as noted by the error bars.

died from nonspecific causes before visible tumor growth occurred. After 2 wk, tumors were visible in all mice injected with either cell line. In concordance with the in vitro growth rate studies, the tumors produced by the parental cells grew faster than those from the vgr-1–transfected CHO cells (data not shown). After 1 mo, or by the time the tumors reached 4 cm in largest diameter, the animals were killed and autopsies were performed.

The tumors produced by both cell types were well localized and encapsulated. However, the tumors had striking differences in gross morphology (Fig. 5). The parental cells produced tumors with a convoluted surface, and they were hemorrhagic, necrotic, and friable (Fig. 5 *A*). In contrast, the CHO-vgr-1 tumors did not have a significant hemorrhagic component, had a smooth surface, and were quite dense, firm, and fibrotic (Fig. 5 *B*).

Histological examination of these tumors further highlighted the differences noted in the gross morphology. Hematoxylin and eosin staining of the CHO tumors showed nests of tumor cells surrounded by necrotic debris, as well as red and white blood cells (Fig. 6 *A*). Similar nests of tumor cells were also seen in the CHO-vgr-1 tumors, but there were no significant areas of necrosis. Moreover, the tumor cells were encompassed by regions of fibrosis, with significant expansion of surrounding connective tissue (Fig. 6 *B*). The tumors induced by the CHO-vgr-1 cells appeared to contain a well-developed vasculature, which in turn supported the growth and development of an organized tissue mass.

Bone and Cartilage Formation in vgr-1 Expressing CHO Tumors

Further histological examination of hematoxylin-eosin–stained tissue sections from CHO-vgr-1 revealed regions of cartilage and bone tissue within portions of the mesenchyme in and around the tumors, accounting for ~20% of the tumor mass (Fig. 6 *C*). These areas contained varying amounts of cartilage and bone, with some consisting solely of cartilage, others containing a mixture of both cartilage and bone, and finally, areas corresponding solely to bone. No bone and cartilage tissue was observed in any of the tumors derived from the parental CHO cells.

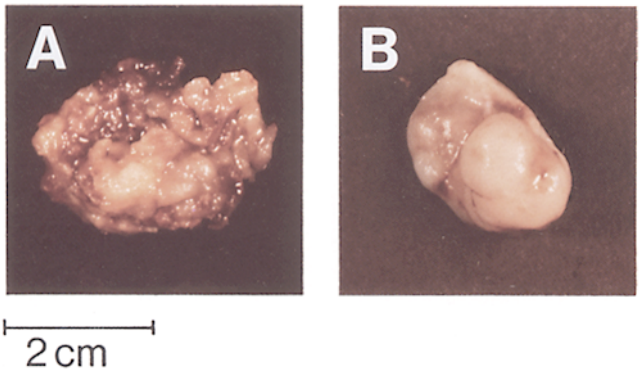

Figure 5. Gross morphology of tumors produced by CHO or CHO-vgr-1 cells. (*A*) A CHO tumor, with convoluted surface and significant hemorrhage, was friable and necrotic. (*B*) A CHO-vgr-1 tumor, with smooth surface and only limited hemorrhage, was firm, dense, and fibrotic. Scale bar indicates the size of the tumors.

To further characterize these areas of bone and cartilage formation, we performed several histochemical and immunohistochemical staining procedures. In Fig. 7, the tumor sections were stained with Alcian blue, which binds to mucopolysaccharides found in cartilage. The CHO tumor sections did not stain with Alcian blue, but only with the counterstain, whereas the CHO-vgr-1 tumors contained extensive regions of blue staining (Fig. 7, *A* and *B*). At higher magnification, these areas appeared morphologically as chondrocytes or hypertrophic chondrocytes (Fig. 7 *C*). An adjacent section was stained by the von Kossa method, and some of these same areas stained black, indicating regions of mineralization. Thus, such areas contained hypertrophic cartilage that had mineralized; if this tumor had been incubated longer in vivo, then this area would presumably have been replaced by bone.

To confirm areas of bone formation within the CHO-vgr-1 tumors, we analyzed different sections using the von Kossa and trichrome staining methods. As shown in Fig. 8, CHO-vgr-1 tumors, but not tumors derived from the parental CHO cells, had areas that stained positively in regions that appeared morphologically as trabecular bone. At a higher magnification, we noted the presence of osteoblasts, osteocytes, and osteoclasts within such areas of trabecular bone.

The regions of cartilage and bone were further defined with immunohistochemical analyses for collagen II, which is specifically deposited in cartilage, and for collagen I and osteocalcin, proteins associated with bone. Portions of the CHO-vgr-1 tumor stained specifically with the collagen II antibody, with such staining apparent in cartilage matrix, but not in areas of apparent bone formation (Fig. 9 *A*). No collagen II staining was detected in the CHO tumors. Other areas that appeared histologically as bone were stained with antibodies for both collagen I and osteocalcin (Fig. 9, *B* and *C*). No such dual collagen I and osteocalcin staining was seen in any region of the CHO tumors. Collagen I staining was not confined to bone in the CHO-vgr-1 tumors, but was also noted within areas of surrounding connective tissue; widespread staining was also noted within the CHO tumors in regions of necrotic debris. Finally, CHO-vgr-1 tumors also had regions that stained with all three antibodies, indicative of cartilage adjacent to bone tissue (Fig. 9 *D*). Collectively, these findings suggest that there had been a recapitulation of endochondral bone formation within these tumors, in which a cartilage template formed initially and was eventually replaced by bone.

We postulated that the vgr-1 secreted by the transfected CHO cells had induced mesenchymal cells of the host animal to differentiate into bone and cartilage. Indeed, mesenchymal cells are known to differentiate into chondroblasts and osteoblasts, whereas CHO cells are not known to differentiate. To prove this hypothesis, we designed a riboprobe for in situ hybridization to distinguish injected CHO cells from host mouse cells. Although both the host and transfected CHO cells expressed endogenous dhfr mRNA, the CHO cells also overexpressed an additional dhfr mRNA derived from the transfected expression vector (45). This latter transcript contained a unique 3′ untranslated region derived from the hepatitis B surface antigen gene. This region served as a riboprobe to specifically identify CHO cells within the tumor samples. As seen in Fig. 10 *A*, the antisense riboprobe hybridized intensely to the nests of CHO-

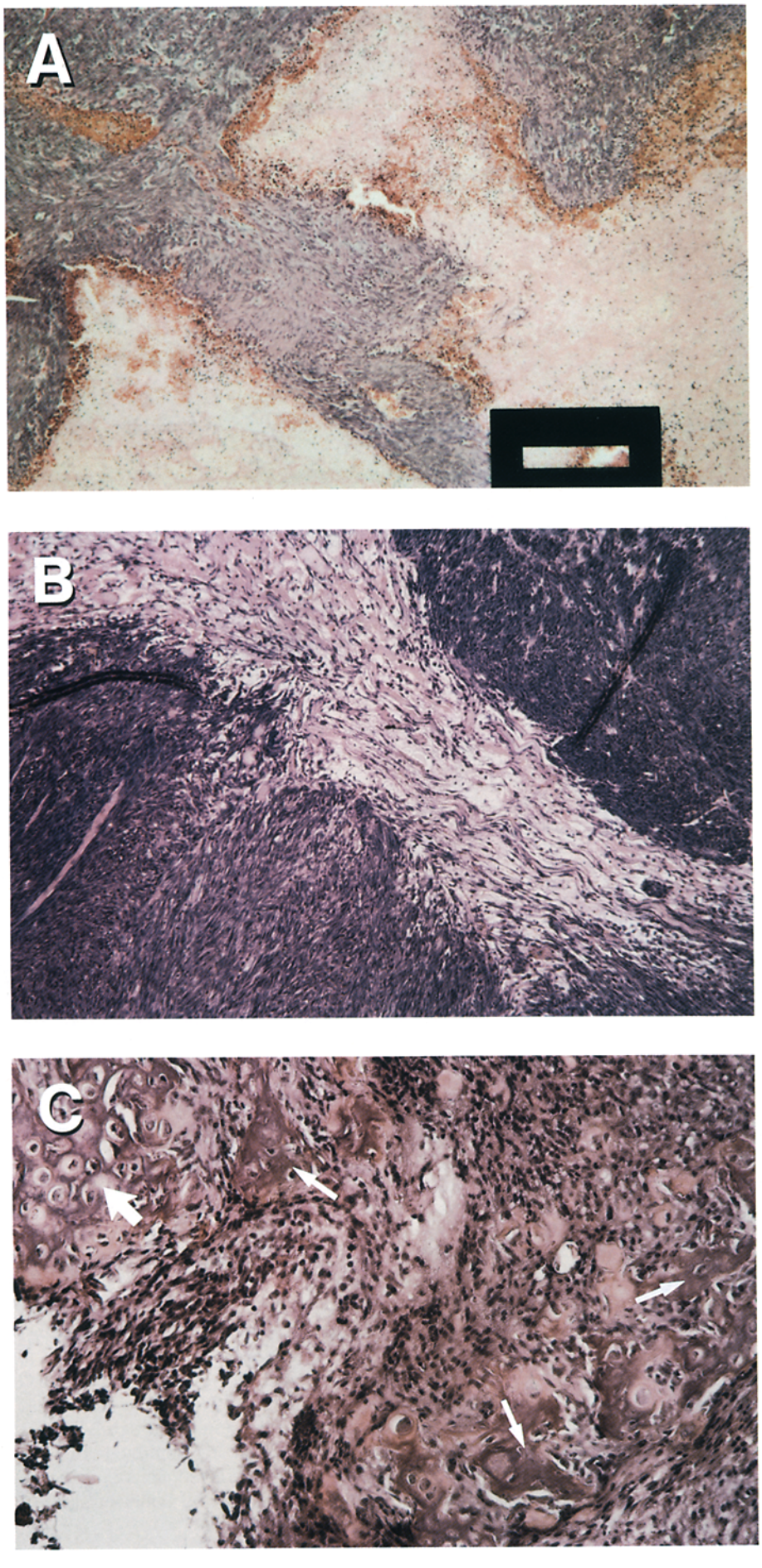

Figure 6. Haematoxylin and eosin staining of tumors. (*A*) Section from a CHO tumor, showing areas of darker stained tumor cells with surrounding hemorrhage (*orange*) and necrosis (*lighter stained pink areas*). Bar, 200 μm. (*B*) Section from a CHO-vgr-1 tumor, showing two regions of darker stained tumor cells separated by connective tissue. (*C*) Section of CHO-vgr-1 tumor showing areas of cartilage (*upper left corner of figure, large arrow*) and bone (*smaller arrows*). Magnification for *A* and *B* is ×10, and *C* is ×20.

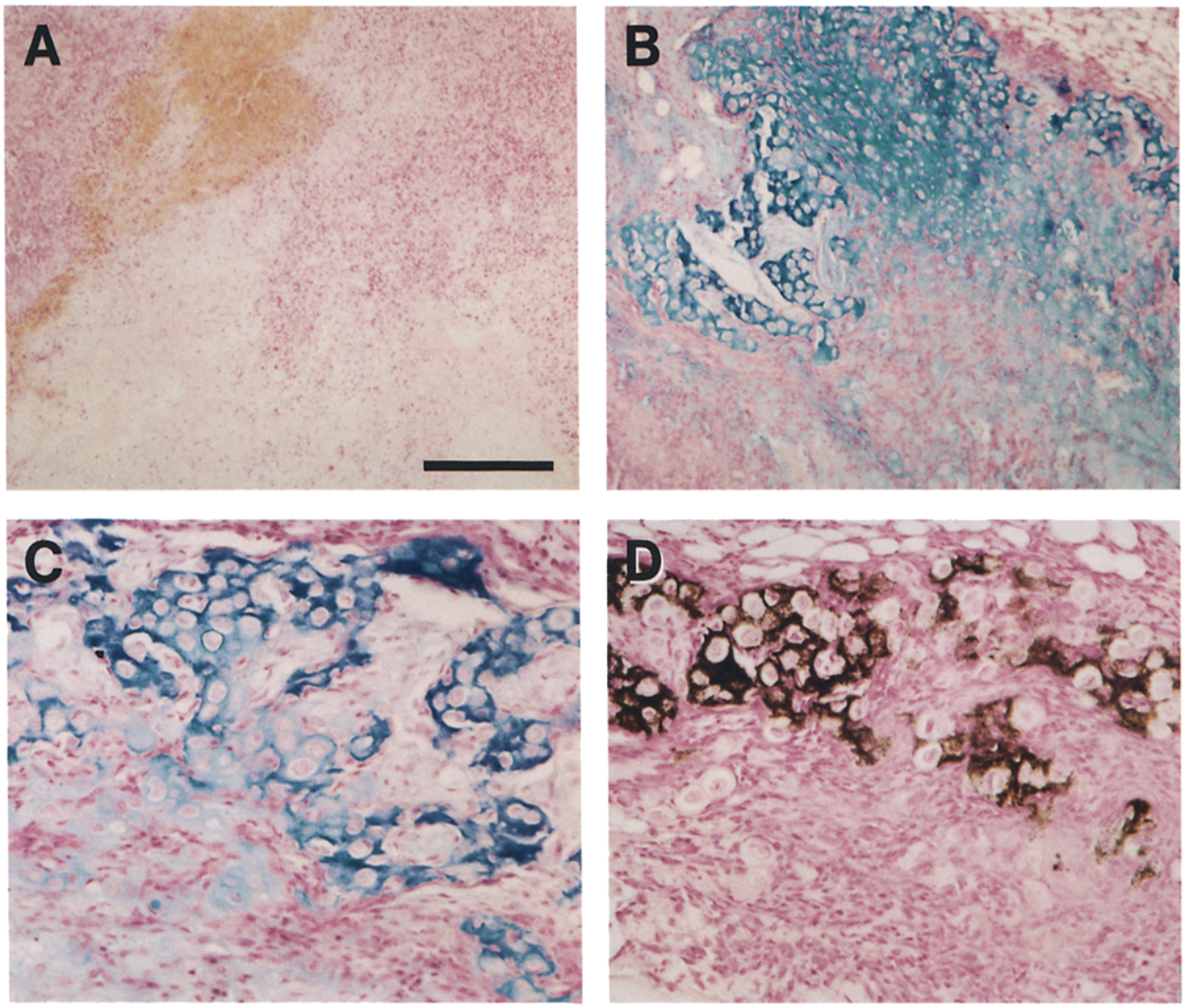

Figure 7. Regions of cartilage within the CHO-vgr-1 tumors. (*A*) CHO tumor stained with Alcian blue and nuclear fast red counterstain, with only the counterstain visualized. CHO cells are present in the upper left corner of the figure, with surrounding necrotic debris and red blood cells (*tan*). Image is seen at ×10. Bar, 200 μm. (*B*) ×10 view of CHO-vgr-1 tumor stained with Alcian blue, with marked areas of intense blue staining the matrix surrounding chondrocytes. (*C*) ×20 view of the Alcian blue staining region shown in *B*. Cell morphology corresponds to chondrocytes and hypertrophic chondrocytes. (*D*) von Kossa stain of an adjacent section, with black areas corresponding to mineralization of some portions of the cartilage.

vgr-1 tumor cells, but did not react with the cells in the cartilage and bone tissue and surrounding mesenchyme at the tumor periphery. Therefore, the cells within these tissues must have arisen from mesenchymal cells of the host animal that had been incorporated into the tumor. A low, uniform background of nonspecific hybridization was seen using the sense strand probe as a negative control (Fig. 10, *C* and *D*). This conclusion was further strengthened by the positive immunostaining for osteocalcin (Fig. 9). This antibody recognizes only mouse but not hamster osteocalcin, confirming that the bone tissue must have originated from mouse.

Discussion

Little is currently known about the function of a distinct subgroup of the TGF-β superfamily consisting of BMP-5, vgr-1/BMP-6, OP-1/BMP-7, and OP-2. We have focused on vgr-1/BMP-6 as a prototype member of this subgroup. The previous finding that vgr-1 mRNA is the only TGF-β superfamily member localized to hypertrophic cartilage suggests that it may play a pivotal role in the transition of cartilage to bone during endochondral bone formation. We report here the generation of vgr-1–specific antibodies and the subsequent immunohistochemical localization of vgr-1 protein to hypertrophic cartilage. Furthermore, we produced stably transfected CHO cells expressing recombinant vgr-1 protein at high levels. Finally, we injected the vgr-1–expressing CHO cells into mice to evaluate the effects of continuous release of vgr-1 in vivo. In contrast to the nontransfected cells, the tumors formed by vgr-1–expressing cells contained extensive areas of fibrosis, with bone and cartilage formation in a pattern that seemed to mimic endochondral bone formation.

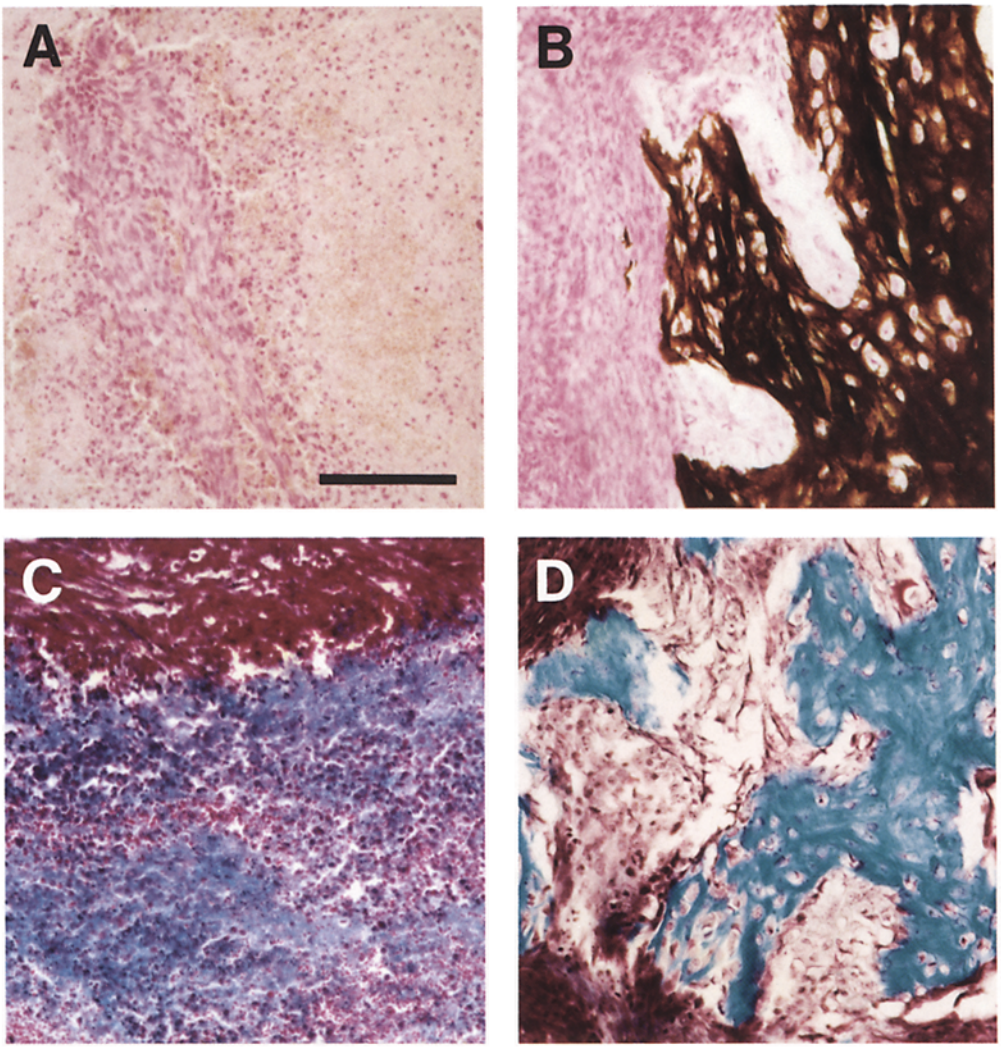

Figure 8. Regions of bone within the CHO-vgr-1 tumors. (*A*) von Kossa stain of CHO-tumor, with only background nuclear fast red stain visualized. CHO cells stain pink, and they are visualized in the left central portion of the figure surrounded by necrotic debris and red blood cells (*staining tan*). (*B*) von Kossa stain of CHO-vgr-1 tumor, with black areas corresponding to regions of trabecular bone. CHO-vgr-1 cells are the pink-stained cells on the left side of the figure. (*C*) Trichrome stain of CHO tumor with no positive staining, and only the Weigert hematoxylin counterstain is visualized. CHO cells are the magenta-stained regions on the upper portion of the figure. (*D*) Trichrome stain of CHO-vgr-1 tumor with intense blue staining of trabecular bone. CHO-vgr-1 cells are the magenta-stained regions in the upper left and lower left portions of the figure. All images are seen at ×20. Bar, 100 μm.

Vgr-1 Expression in Hypertrophic Cartilage

Previous studies have localized vgr-1 expression in the developing mouse using both in situ hybridization and immunohistochemistry (21, 29, 50). The former studies established the expression of vgr-1 mRNA in the central nervous system, suprabasal layer of the epidermis and other epithelial structures, and in hypertrophic cartilage. However, using immunohistochemistry, vgr-1 protein was found only in the central nervous system and epithelial structures, but not in hypertrophic cartilage, leading to the suggestion that the mRNA may not be translated in the latter tissue (50). We now report that vgr-1 mRNA is indeed translated into protein in hypertophic chondrocytes, as assessed by immunohistochemical staining using our vgr-1 antibody. The antibody staining is highly localized in the matrix surrounding the hypertrophic chondrocytes. This staining pattern strongly suggests that the secreted vgr-1 has a very limited diffusion range and that the hypertrophic cartilage matrix serves as a reservoir for this TGF-β superfamily member.

Vgr-1 was immunolocalized to hypertrophic cartilage solely using an antibody against the mature, carboxy-terminal portion of the protein. In contrast, both Wall et al. (50) and ourselves were unable to detect protein expression in this tissue using an antibody directed against the vgr-1 precursor segment. The reason for this inability remains unclear. One possibility is that the precursor region has acquired an altered conformation, either naturally or as a result of the treatment procedure, that renders it inaccessible to the antibody. If this were the case, then this modification must be different from that in epithelial structures and in the central nervous system, where the vgr-1 precursor antibody was used successfully. Alternatively, the vgr-1 precursor segment may be proteolytically degraded in hypertrophic cartilage. This would resemble the proteolytic activation of TGF-β1 in situ after irradiation, which is accompanied by a strong decrease in immunostaining using a precursor-specific antibody (2). Such vgr-1 precursor segment degradation could, in turn, provide higher accessibility of mature vgr-1 for its receptor, as in the case of TGF-β.

Recombinant Expression of vgr-1 Protein and Biological Activity In Vivo

To evaluate the biological functions of murine vgr-1, we generated an efficient expression plasmid to overexpress recombinant protein. CHO cells stably transfected with this vector synthesized and secreted high levels of recombinant vgr-1 protein, approximately half of which had undergone the predicted proteolytic cleavage. The transfected cells grew

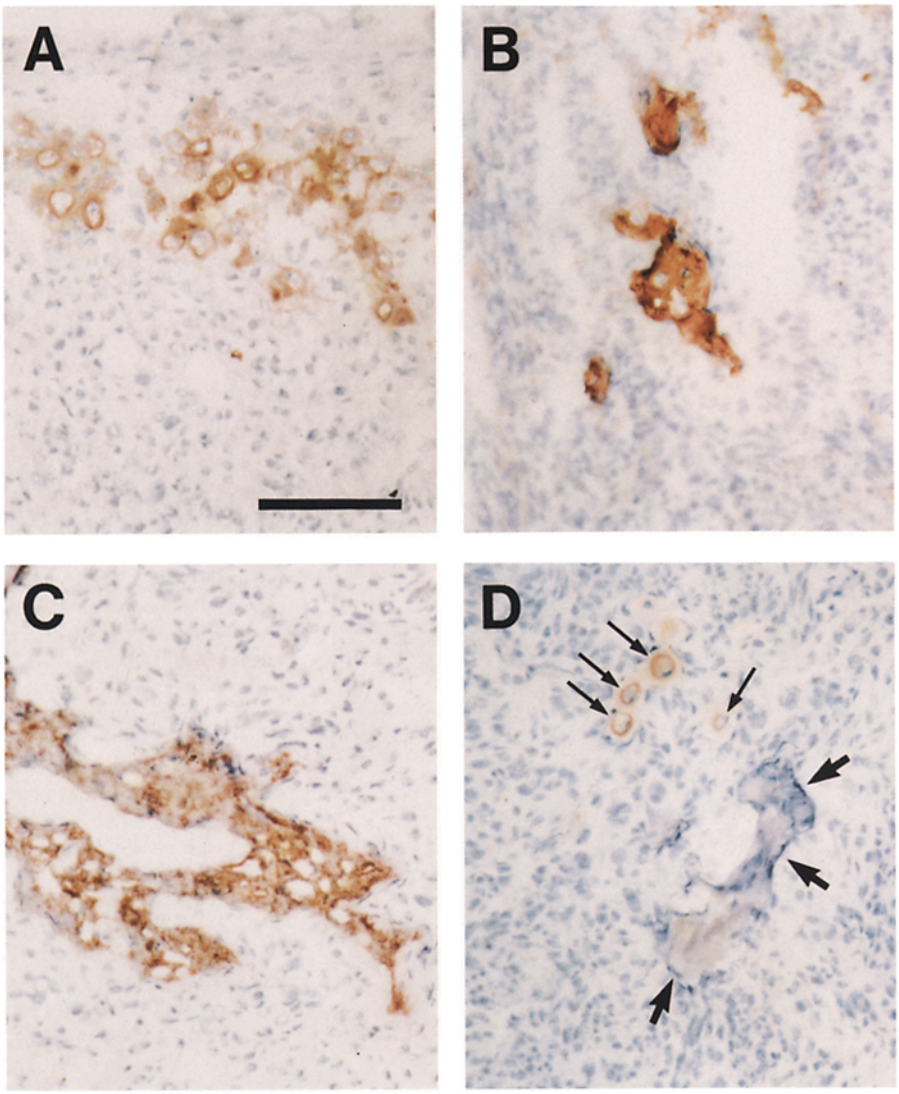

Figure 9. Immunohistochemistry of bone and cartilage in CHO- vgr-1 tumors. (*A*) CHO-vgr-1 tumor section stained with a collagen II antibody, identifying areas of cartilage formation (*brown*). (*B*) CHO-vgr-1 tumor section stained with a collagen I antibody, identifying regions corresponding to bone (*brown*). (*C*) CHO-vgr-1 tumor section stained with an osteocalcin antibody, identifying regions corresponding to bone (*brown*). (*D*) CHO-vgr-1 tumor section that contains an area that appears morphologically as bone (*large arrows*), and stained with collagen II antibody, identifying chondrocytes that are adjacent to bone tissue (*circular brown areas noted by smaller arrows*). All views are ×20. Bar, 100 μm.

slower than the parental cells, but otherwise exhibited no significant differences when characterized in vitro.

To assay the biological activity of vgr-1 in vivo, we introduced the CHO-vgr-1 transfectants directly into mice via a subcutaneous injection, rather than first purifying recombinant protein from conditioned media of the CHO-vgr-1 cells. Previous studies have documented that CHO cells form localized tumors when injected subcutaneously (13), and we reasoned that the transfected cells would act as a depot source of vgr-1 by continuously releasing the recombinant protein within the tumor. As expected, injection of the CHO-vgr-1 stable transfectants in nude mice induced tumor formation, as did the parental cells. However, the CHO-vgr-1 tumors showed a striking increase in surrounding connective tissue and exhibited bone and cartilage formation. Some areas showed only cartilage or trabecular bone; others contained bone intimately associated with adjacent areas of cartilage, or contained areas of mineralized cartilage. Taken collectively, these findings suggest recapitulation of endochondral bone formation, in which a cartilage template is first formed, and is later replaced by mineralized bone.

Another fundamental difference between the tumors induced by the CHO cells as opposed to the CHO-vgr-1 transfectants was that the parental cells produced tumors lacking any organized vascular supply. Thus, overgrowth of these cells resulted in hemorrhagic, necrotic debris, and the tumors were unable to support development of an organized tissue mass. By contrast, the CHO-vgr-1 cells formed tumors with a well-delineated vascular supply, and thereby supported development of well-organized tumor masses, with profusion of connective tissue and differentiation of cartilage and bone. During endochondral bone formation, angiogenesis in hypertrophic cartilage is critical for mineralization and subsequent bone formation. The endogenous localization of vgr-1 to the site of angiogenesis in hypertrophic cartilage suggests that this factor may mediate new vessel formation.

The cellular elements of fibrosis and endochondral bone formation within the CHO-vgr-1 tumors did not appear to have arisen directly from the CHO cells, but instead from the effects of secreted vgr-1 on surrounding host mesenchymal cells. Several lines of evidence support this hypothesis. First, the connective tissue, cartilage, and bone did not hybridize with a riboprobe that specifically identified the transfected CHO cells. Second, CHO cells are not known to differentiate

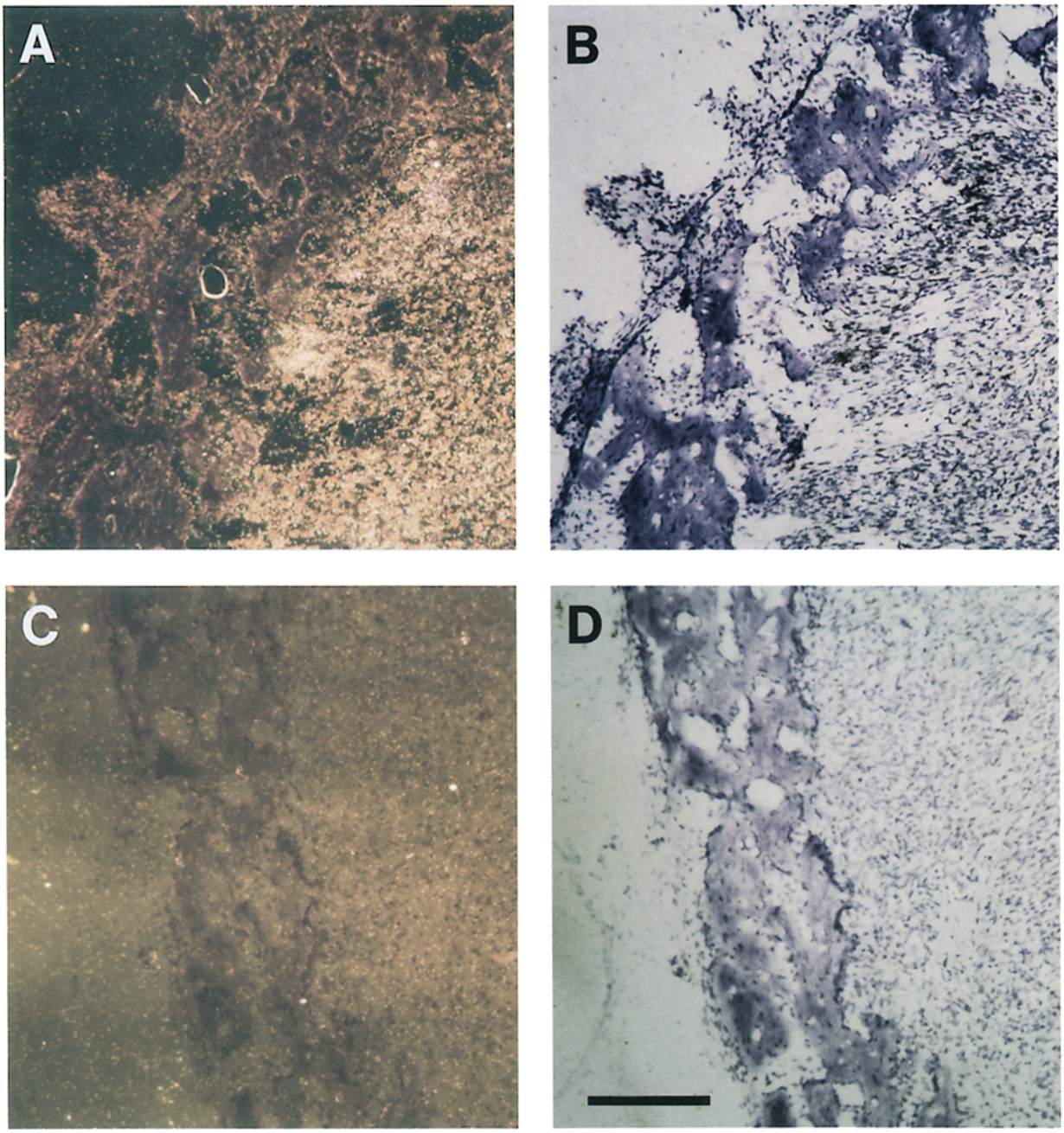

Figure 10. In situ hybridizations to define CHO cells within the tumors. (*A*) Dark-field microscopy of section from a CHO-vgr-1 tumor that has been hybridized with an antisense riboprobe directed against the 3′ untranslated region of hepatitis B surface antigen. This probe corresponds to part of the dhfr transcript generated from the expression vector transfected into the CHO cells, and most importantly, it identifies an mRNA specific to the CHO cells. White grains correspond to probe that has hybridized to CHO-vgr-1 cells. Note that the bone and surrounding mesenchyme lack significant hybridization. (*B*) Bright-field view of section shown in *A*. The darker staining regions correspond to trabecular bone. (*C*) Dark-field microscopy of section from a CHO-vgr-1 tumor that has been hybridized with a sense riboprobe to hepatitis B surface antigen, serving as a negative control. A low level of background hybridization is shown uniformly throughout the section. (*D*) Bright-field view of the section shown in *C*. All views are ×10. Bar, 200 μm.

in vitro or in vivo, making it unlikely that the vgr-1–transfected CHO cells differentiated into osteoblasts or chondrocytes. In fact, the transfected cells exhibited no such differentiation when evaluated in vitro. Third, the bone matrix within the CHO-vgr-1 tumors stained positively using a monoclonal antibody specific for mouse osteocalcin that does not cross-react with rat or hamster osteocalcin, further substantiating our conclusion that the ectopic bone did not originate from hamster cells. Finally, conditioned media from CHO-vgr-1 cells, but not from CHO cells, also induced ectopic bone formation when injected intramuscularly (Kirk, M., and S. E. Gitelman, unpublished results).

Vgr-1 secreted by the CHO-vgr-1 tumors appeared to have acted only locally within these animals. We have not devel-

oped an assay to measure serum levels of vgr-1, and thus have not formally tested if these animals contained significant circulating levels of this factor. However, analysis of long bones near the site of the tumor showed no changes as compared to those of the control animals, and extensive autopsies revealed no significant changes in any other major organs.

Possible Mechanisms of Vgr-1 Action

Our findings indicate that recombinant vgr-1 protein was sufficient to induce fibrosis and bone and cartilage formation in vivo. Yet, the complexity of such an in vivo study makes it difficult to pinpoint the specific primary actions directly attributable to vgr-1, as opposed to secondary actions mediated through other factors. One important function of vgr-1, at least in the context of this study, may be as a chemoattractant to bring various cell types to the tumor, including mesenchymal precursors. Alternatively, vgr-1 may act as a mitogen to increase the number of various host cells already present in or near the tumor. In fact, several other members of the TGF-β superfamily can serve as chemoattractants or mitogens for a variety of cell types, including mesenchymal cells, fibroblasts, osteoblasts, neutrophils, monocytes, epithelial cells, and endothelial cells (for examples, see references 19, 39, 42, 58). The most widely studied factor from this standpoint has been TGF-β1. Injection of recombinant TGF-β1 into newborn mice and chicken chorioallantoic membrane induces a granulation tissue response, with inflammation, fibrosis, and angiogenesis (42, 58). The hypercellular lesions in the chicken study resulted not from cellular proliferation, but from enhanced cell migration through chemotaxis (58). Only limited studies have been conducted with the BMPs, with BMP-3 and BMP-4 chemotactic for monocytes in vitro (9). Further studies are needed to determine if vgr-1 also serves as a chemoattractant and/or mitogen, and if vgr-1's actions in this regard are distinguishable from that of other members of the TGF-β superfamily. Vgr-1 does not alter the growth rate of two pluripotent mesenchymal cell lines in vitro, suggesting that it may not function as a mitogen in vivo (Gitelman, S. E., J. Q. Ye, and R. Derynck, unpublished results).

The influx of additional host cells into the tumor site adds another layer of complexity in characterizing the primary actions of vgr-1. Each of these cell types may release additional factors into the tumor area, such as other TGF-β superfamily members, local growth factors, cytokines, or various extracellular matrix proteins. Vgr-1 may act in a paracrine fashion to stimulate production and release of such factors from these neighboring host cells, and may also act in concert with these factors to induce the fibrotic changes and endochondral bone formation noted within the CHO-vgr-1 tumors.

Role of TGF-β Superfamily in Endochondral Bone Formation

Several members of the TGF-β superfamily have now been shown to induce endochondral bone formation when injected in vivo. TGF-β1 and TGF-β2 induce endochondral bone formation when introduced subperiosteally or at a fracture site, but not at a site that is not anatomically connected to bone (4, 23, 32, 35). In contrast, BMP-2, -3, -4, -7, and now vgr-1 have the ability to induce ectopic bone formation when injected intramuscularly or subcutaneously (17, 28, 43, 51, 54). Such findings suggest that these BMPs may act on a less differentiated mesenchymal precursor than TGF-β during endochondral bone formation. The findings also imply functional redundancy among these factors, yet specificity appears to reside in the spatially and temporally distinctive patterns of their expression (for an example, see reference 31).

In all other studies, a recombinant factor has been introduced in vivo as a purified protein delivered within an inert carrier. Our study is the first to have been conducted with direct injection of CHO cells that continuously release recombinant protein. As a result, comparison of vgr-1's potency with that of the other TGF-β related factors is not yet possible, and awaits purification of recombinant vgr-1 from conditioned media.

Definition of the specific role of individual TGF-β superfamily members in endochondral bone formation awaits more refined studies, both in vitro and in vivo. The present study entailed overexpression of vgr-1 in an ectopic location, and demonstrated that vgr-1 had the ability to initiate mesenchymal differentiation along the endochondral bone pathway. To further define the function of this factor during normal bone and cartilage development, it will be important to manipulate the expression of vgr-1 and its receptor within hypertrophic cartilage, vgr-1's endogenous site of production.

We thank Ilse Sauerwald for her assistance in fixation and sectioning of tissues and histological staining. We also acknowledge the generous help of Drs. Päivi Miettinen, Synthia Mellon, and Henry Rodriguez with the in situ hybridizations. We appreciate the interest and support of Arnold Kahn throughout the course of this work.

This work was supported by grants from the Lawson Wilkens Pediatric Endocrine Society (Genentech Clinical Scholar's Award) and National Institutes of Health (NIH) grant 1 K08 AR01897-01 to S. Gitelman, and NIH grants R01-AR41126 to R. Derynck, and P50DE10306 to the Research Center in Oral Biology.

Received for publication 5 January 1994 and in revised form 14 May 1994.

References

1. Asahina, I., T. K. Sampath, I. Nishimura, and P. V. Hauschka. 1993. Human osteogenic protein-1 induces both chondroblastic and osteoblastic differentiation of osteoprogenitor cells derived from newborn rat calvaria. *J. Cell Biol.* 123:921–933.
2. Barcellos-Hoff, M.-H., R. Derynck, M. L.-S. Tsang, and J. A. Weatherbee. 1994. Transforming growth factor-β activation in irradiated murine mammary gland. *J. Clin. Invest.* 93:892–899.
3. Basler, K., T. Edlund, T. M. Jessell, and T. Yamada. 1993. Control of cell pattern in the neural tube: regulation of cell differentiation by dorsalin-1, a novel TGF-β family member. *Cell.* 73:687–702.
4. Beck, L. S., L. Deguzman, W. P. Lee, Y. Xu, L. A. McFatridge, N. A. Gillett, and E. P. Amento. 1991. TGF-β1 induces bone closure of skull defects. *J. Bone Miner. Res.* 6:1257–1265.
5. Celeste, A. J., J. A. Iannazzi, R. C. Taylor, R. M. Hewick, V. Rosen, E. A. Wang, and J. M. Wozney. 1990. Identification of transforming growth factor β family members present in bone-inductive protein purified from bovine bone. *Proc. Natl. Acad. Sci. USA.* 87:9843–9847.
6. Chen, T. L., R. L. Bates, A. Dudley, R. G. Hammonds, and E. P. Amento. 1991. Bone Morphogenetic protein-2b stimulation of growth and osteogenic phenotypes in rat osteoblast-like cells: comparison with TGF-β1. *J. Bone Miner. Res.* 6:1387–1393.
7. Chomczynski, P., and N. Sacchi. 1987. Single-step method of RNA isolation by acid guanidium thiocyanate-phenol-chloroform extraction. *Anal. Biochem.* 162:156–159.
8. Clark, G. 1981. Staining Procedures. 4th ed. Williams and Wilkins, Baltimore.
9. Cunningham, N. S., V. Paralkar, and A. H. Reddi. 1992. Osteogenin and recombinant bone morphogenetic protein 2B are chemotactic for human monocytes and stimulate transforming growth factor β1 mRNA expression. *Proc. Natl. Acad. Sci. USA.* 89:11740–11744.
10. Derynck, R. 1994. Transforming growth factor β. *In* The Cytokine Handbook. 2nd ed. A. Thompson, editor. Academic Press, Boston. pp. 319–342.

11. Derynck, R., P. B. Lindquist, A. Lee, D. Wen, J. Tamm, J. L. Graycar, L. Rhee, A. J. Mason, D. A. Miller, R. J. Coffey, et al. A new type of transforming growth factor β, TGF-β3. *EMBO (Eur. Mol. Biol. Organ.) J.* 7:3737–3743.
12. Doctor, J. S., P. D. Jackson, K. E. Rashka, M. Visalli, and F. M. Hoffmann. 1992. Sequence, biochemical characterization, and developmental expression of a new member of the TGF-β superfamily in *Drosophila melanogaster. Dev. Biol.* 151:491–505.
13. Esko, J. D., K. S. Rostand, and J. L. Weinke. 1988. Tumor formation dependent on proteoglycan biosynthesis. *Science (Wash. DC).* 241:1092–1095.
14. Gazit, D., R. Ebner, A. J. Kahn, and R. Derynck. 1993. Modulation of expression and cell surface binding of members of the transforming growth factor-β superfamily during retinoic acid-induced osteoblastic differentiation of multipotential mesenchymal cells. *Mol. Endocrinol.* 7:189–198.
15. Gorman, C., R. Padmanabhn, and B. H. Howard. 1983. High efficiency DNA-mediated transformation of primate cells. *Science (Wash. DC).* 221:551–553.
16. Green, N., H. Alexander, A. Olson, S. Alexander, T. M. Shinnick, J. G. Sutcliffe, and R. A. Lerner. 1982. Immunogenic structure of the influenza virus hemagglutinin. *Cell.* 28:477–487.
17. Hammonds, R. G., R. Schwall, A. Dudley, C. Lai, L. Berkemeier, N. Cunningham, A. H. Reddi, W. I. Wood, and A. J. Mason. 1991. Bone-inducing activity of mature BMP-2b produced from a hybrid BMP-2a/2b precursor. *Mol. Endocrinol.* 4:149–155.
18. Hiraki, Y., H. Inoue, C. Shigeno, Y. Sanma, H. Bentz, D. M. Rosen, A. Asada, and F. Suzuki. 1991. Bone Morphogenetic Proteins (BMP-2 and BMP-3) promote growth and expression of the differentiated phenotype of rabbit chondrocytes and osteoblastic MC3T3-E1 cells in vitro. *J. Bone Miner. Res.* 6:1373–1385.
19. Hughes, F. J., J. E. Aubin, and J. N. M. Heersche. 1992. Differential chemotactic responses of different populations of fetal rat calvaria cells to platelet-derived growth factor and transforming growth factor β. *Bone Miner.* 19:63–74.
20. Jessell, T. M., and D. A. Melton. 1992. Diffusible factors in vertebrate embryonic induction. *Cell.* 68:257–270.
21. Jones, C. M., K. M. Lyons, and B. L. M. Hogan. 1991. Involvement of bone morphogenetic protein-4 (BMP-4) and vgr-1 in morphogenesis and neurogenesis in the mouse. *Development (Camb.).* 111:531–542.
22. Jones, C. M., D. Simon-Chazottes, J.-L. Guenet, and B. L. M. Hogan. 1992. Isolation of Vgr-2, a novel member of the transforming growth factor-β-related gene family. *Mol. Endocrinol.* 6:1961–1968.
23. Joyce, M. E., A. B. Roberts, M. B. Sporn, and M. E. Bolander. 1990. Transforming growth factor-β and the initiation of chondrogenesis and osteogenesis in the rat femur. *J. Cell Biol.* 110:2195–2207.
24. Katagiri, T., A. Yamaguchi, T. Ikeda, S. Yoshiki, J. M. Wozney, V. Rosen, E. A. Wang, H. Tanaka, S. Omura, and T. Suda. 1990. The non-osteogenic mouse pluripotent cell line, C3H10T1/2, is induced to differentiate into osteoblastic cells by recombinant human bone morphogenetic protein-2. *Biochem. Biophys. Res. Commun.* 172:295–299.
25. Deleted in proof.
26. Kozak, M. 1987. An analysis of 5′-noncoding sequence from 699 vertebrate messenger RNAs. *Nucleic Acids Res.* 15:8125–8148.
27. Lee, S. J. 1990. Identification of a novel member (GDF-1) of the transforming growth factor-β superfamily. *Mol. Endocrinol.* 4:1034–1040.
28. Luyten, F. P., N. S. Cunningham, S. Ma, N. Muthukumaran, R. G. Hammonds, W. B. Nevins, W. I. Woods, and A. H. Reddi. 1989. Purification and partial amino acid sequence of osteogenin, a protein initiating bone differentiation. *J. Biol. Chem.* 264:13377–13380.
29. Lyons, K., J. L. Graycar, A. Lee, S. Hashmi, P. B. Lindquist, E. Y. Chen, B. L. M. Hogan, and R. Derynck. 1989. Vgr-1, a mammalian gene related to *Xenopus* Vg-1, is a member of the transforming growth factor beta gene superfamily. *Proc. Natl. Acad. Sci. USA.* 86:4554–4558.
30. Lyons, K. M., C. M. Jones, and B. L. M. Hogan. 1991. The DVR gene family in embryonic development. *Trends Genet.* 7:408–412.
31. Lyons, K. M., R. W. Pelton, and B. L. M. Hogan. 1989. Patterns of expression of murine Vgr-1 and BMP-2 RNA suggest that transforming growth factor-beta-like genes coordinately regulate aspects of embryonic development. *Genes & Dev.* 3:1657–1668.
32. Marcelli, C , A. J. Yates, and G. R. Mundy. 1990. In vivo effects of human recombinant transforming growth factor β on bone turnover in normal mice. *J. Bone Miner. Res.* 5:1087–1096.
33. McPherron, A. C., and S.-J. Lee. 1993. GDF-3 and GDF-9: two new members of the transforming growth factor-β superfamily containing a novel pattern of cysteines. *J. Biol. Chem.* 268:3444–3449.
34. Miettinen, P., and K. Heikinheimo. 1992. Transforming growth factor-alpha and insulin gene expression in human fetal pancreas. *Development (Camb.).* 114:833–840.
35. Noda, M., and J. J. Camilliere. 1989. In vivo stimulation of bone formation by transforming growth factor β. *Endocrinology.* 124:2991–2994.
36. Ozkaynak, E., D. C. Rueger, E. A. Drier, C. Corbett, R. J. Ridge, T. K. Sampath, and H. Opperman. 1990. OP-1 cDNA encodes an osteogenic protein in the TGF-β family. *EMBO (Eur. Mol. Biol. Organ.) J.* 9:2085–2093.
37. Ozkaynak, E., P. N. J. Schnegelsberg, D. F. Jin, G. M. Clifford, F. D. Warren, E. A. Drier, and H. Oppermann. 1992. Osteogenic protein-2. *J. Biol. Chem.* 267:25220–25227.
38. Padgett, R. W., R. D. Johnston, and W. M. Gelbart. 1987. A transcript from a *Drosophila* pattern gene predicts a protein homologous to the transforming growth factor-beta family. *Nature (Lond.).* 325:81–84.
39. Pfeilschifter, J., O. Wolf, A. Naumann, H. W. Minne, G. R. Mundy, and R. Ziegler. 1990. Chemotactic response of osteoblastlike cells to transforming growth factor β. *J. Bone Miner Res.* 5:825–830.
40. Reddi, A. H., and C. Huggins. 1972. Biochemical sequences in the transformation of normal fibroblasts in adolescent rats. *Proc. Natl. Acad. Sci. USA.* 69:1601–1605.
41. Roberts, A. B., and M. B. Sporn. 1990. The transforming growth factor-betas. *In* Handbook of Experimental Pharmacology. Peptide Growth Factors and their Receptors. Springer-Verlag, Heidelberg, Germany. M. B. Sporn and A. B. Roberts, editors. pp. 419–472.
42. Roberts, A. B., M. B. Sporn, R. K. Assoian, J. M. Smith, N. S. Roche, L. M. Wakefield, U. I. Heine, L. A. Liotta, V. Falanga, J. H. Kehrl, and A. S. Fauci. 1986. Transforming growth factor β: rapid induction of fibrosis and angiogenesis in vivo and stimulation of collagen formation in vitro. *Proc. Natl. Acad. Sci. USA.* 83:4167–4171.
43. Sampath, T. K., J. C. Maliakal, P. V. Hauschka, W. K. Jones, H. Sasak, R. F. Tucker, K. H. White, J. E. Coughlin, M. M. Tucker, R. H. L. Pang, et al. Recombinant human osteogenic protein-1 (hOP-1) induces new bone formation in vivo with a specific activity comparable with natural bovine osteogenic protein and stimulates osteoblast proliferation and differentiation in vitro. *J. Biol. Chem.* 267:20352–20362.
44. Sanger, F., S. Nicklen, and A. R. Coulson. 1977. DNA sequencing with chain-terminating inhibitors. *Proc. Natl. Acad. Sci. USA.* 74:5463–5467.
45. Simonsen, C. C., and A. D. Levinson. 1983. The isolation and expression of an altered mouse dihydrofolate reductase cDNA. *Proc. Natl. Acad. Sci. USA.* 80:2495–2499.
46. Urist, M. R. 1965. Bone: formation by autoinduction. *Science (Wash. DC).* 150:893–899.
47. Urlaub, G., and L. A. Chasin. 1980. Isolation of chinese hamster cell mutants deficient in dihydrofolate reductase activity. *Proc. Natl. Acad. Sci. USA.* 77:4216–4220.
48. von Heijne, G. 1986. A new method for predicting signal sequence cleavage sites. *Nucleic Acids Res.* 14:4683–4690.
49. Vukicevic, S., F. Luyten, and A. H. Reddi. 1989. Stimulation of the expression of osteogenic and chondrogenic phenotypes in vitro by osteogenin. *Proc. Natl. Acad. Sci. USA.* 86:8793–8797.
50. Wall, N. A., M. Blessing, C. V. E. Wright, and B. L. M. Hogan. 1993. Biosynthesis and in vivo localization of the decapentaplegic-Vg-related protein, DVR-6 (bone morphogenetic protein-6). *J. Cell Biol.* 120: 493–502.
51. Wang, E. A., V. Rosen, J. S. D'Alessandro, M. Bauduy, P. Cordes, T. Harada, D. I. Israel, R. M. Hewick, K. M. Kerns, P. LaPan, et al. Recombinant human bone morphogenetic protein induces bone formation. *Proc. Natl. Acad. Sci. USA.* 87:2220–2224.
52. Wigler, M., R. Sweet, G. K. Sim, B. Wold, A. Pellicer, E. Lacy, T. Maniatis, S. Silverstein, and R. Axel. 1979. Transformation of mammalian cells with genes from prokaryotes and eukaryotes. *Cell.* 16:777–785.
53. Wood, W. I., G. Cachianes, W. I. Henzel, J. A. Winslow, S. A. Spencer, R. Helmiss, J. L. Martin, and R. C. Baxter. 1988. Cloning and expression of the growth hormone-dependent insulin-like growth factor binding protein. *Mol. Endocrinol.* 2:1176–1185.
54. Wozney, J., V. Rosen, A. J. Celeste, L. M. Mitsock, M. J. Whitters, R. W. Kriz, R. M. Hewick, and E. A. Wang. 1988. Novel regulators of bone formation: molecular clones and activities. *Science (Wash. DC).* 242:1528–1534.
55. Wozney, J. M. 1992. The bone morphogenetic protein family and osteogenesis. *Mol. Reprod. Dev.* 32:160–167.
56. Yamaguchi, A., and A. J. Kahn. 1991. Clonal osteogenic cell lines express myogenic and adipocytic developmental potential. *Calcif. Tissue Int.* 49: 221–225.
57. Yamaguchi, A., T. Katagiri, T. Ikeda, J. M. Wozney, V. Rosen, E. A. Wang, A. J. Kahn, T. Suda, and S. Yoshiki. 1991. Recombinant human bone morphogenetic protein-2 stimulates osteoblastic maturation and inhibits myogenic differentiation in vitro. *J. Cell Biol.* 113:681–687.
58. Yang, E. Y., and H. L. Moses. 1990. Transforming growth factor β1-induced changes in cell migration, proliferation, and angiogenesis in the chicken chorioallantoic membrane. *J. Cell Biol.* 111:731–741.
59. Zhou, X., H. Sasaki, L. Lowe, B. L. Hogan, and M. R. Kuehn. 1993. Nodal is a novel TGF-beta-like gene expressed in the mouse node during gastrulation. *Nature (Lond.).* 361:543–547.